

However, the absence of abundant lithic assemblages at these Hata archaeology sites requires explanation.

At the nearby Gona site, abundant Oldowan tools were made and discarded immediately adjacent to cobble conglomerates that offered excellent, easily accessible raw materials for stone-tool manufacture. It has been suggested that the surprisingly advanced character of this earliest Oldowan technology was conditioned by the ease of access to appropriate fine-grained raw materials at Gona (10). Along the Karari escarpment at Koobi Fora (13), the basin margin at Fejej (14), and the lake margin at Olduvai Gorge (12), hominids also had easy access to nearby outcrops of raw material. In contrast, the diminutive nature of the Oldowan assemblages in the lower Omo [made on tiny quartz pebbles (15)] was apparently conditioned by a lack of available large clasts.

The situation on the Hata lake margin was even more difficult for early toolmakers. Here, raw materials were not readily available because of the absence of streams capable of carrying even pebbles. There were no nearby basalt outcrops. The absence of locally available raw material on the flat featureless Hata lake margin may explain the absence of lithic artifact concentrations. The bone modification evidence demonstrates that early hominids were transporting stone to the site of carcass manipulation. The paucity of evidence for lithic artifact abandonment at these sites suggests that these early hominids may have been curating their tools (cores and flakes) with foresight for subsequent use. Indications of tool curation by later hominids have been found at the more recent Pleistocene sites of Koobi Fora [Karari escarpment versus Ileret (13)] and Swartkrans [polished bone tools in a single repository (16)].

Additional research into the Hata beds may allow a determination of whether the butchery is related to hunting or scavenging. The Bouri discoveries show that the earliest Pliocene archaeological assemblages and their landscape patterning are strongly conditioned by the availability of raw material. They demonstrate that a major function of the earliest known tools was meat and marrow processing of large carcasses. Finally, they extend this pattern of butchery by hominids well into the Pliocene.

References and Notes

1. B. Asfaw et al., *Science* **284**, xxx (1999).
2. N. J. Hayward and C. J. Ebinger, *Tectonics* **15**, 244 (1996).
3. J. E. Kalb et al., *Nature* **298**, 17 (1982). Eleven years later, J. E. Kalb et al. [*Newsl. Stratigr.* **29**, 21 (1993)] followed Clark et al. (4) in reversing Daka/Bodo Member order.
4. J. D. Clark et al., *Nature* **307**, 423 (1984).
5. J. D. Clark et al., *Science* **264**, 1907 (1994).
6. P. R. Renne, G. WoldeGabriel, W. K. Hart, G. Heiken, T. D. White, *Geol. Soc. Am. Bull.*, in press.
7. The age of this standard is now known to be slightly older [28.02 Ma (17)], but comparison with previous data (for example, from the Gona) is facilitated by

retaining the standard age of 27.84 Ma. A table of the Ar isotopic data is available at www.sciencemag.org/feature/data/991110.shl.

8. F. J. Hilgen, *Earth Planet. Sci. Lett.* **107**, 249 (1991).
9. The sedimentation rate inferred is conservative because comparison of the $^{40}\text{Ar}/^{39}\text{Ar}$ age with the age of 2.6 Ma (8) for the Gauss/Matuyama boundary more properly requires the use of the older age of the standard (28.02 Ma) and indicates an ~10% greater sedimentation rate.
10. S. Semaw et al., *Nature* **385**, 333 (1997).
11. T. D. White, *Prehistoric Cannibalism at Mancos SMTUMR-2346* (Princeton Univ. Press, Princeton, NJ, 1992); L. R. Binford, *Bones: Ancient Men and Modern Myths* (Academic Press, New York, 1981); R. J. Blumenshine, *J. Hum. Evol.* **29**, 21 (1995); S. D. Capaldo and R. J. Blumenshine, *Am. Antiq.* **59**, 724 (1994).
12. R. J. Blumenshine and F. T. Masao, *J. Hum. Evol.* **21**, 451 (1991).
13. G. L. Isaac et al., *Koobi Fora Research Project Volume 5: Plio-Pleistocene Archaeology* (Clarendon, Oxford, 1997).
14. B. Asfaw et al., *J. Hum. Evol.* **21**, 137 (1991).
15. F. C. Howell, P. Haeserts, J. de Heinzelin, *ibid.* **16**, 665 (1987).
16. C. K. Brain, Ed., *Swartkrans: A Cave's Chronicle of Early Man*, vol. 8 of *Transvaal Museum Monograph Series* (Transvaal Museum, Pretoria, 1993).
17. P. R. Renne et al., *Chem. Geol.* **145**, 117 (1998).
18. The Middle Awash paleoanthropological project is multinational (13 countries), with interdisciplinary research codirected by B. Asfaw, Y. Beyene, J. D. Clark, T. D. White, and G. WoldeGabriel. The research re-

ported here was supported by NSF, the Ann and Gordon Getty Foundation (Berkeley Geochronology Center), and the Institute of Geophysics and Planetary Physics of the University of California and the Earth Environmental Sciences Division at Los Alamos National Laboratory. Additional contributions were made by the Graduate School, the Office for Advancement of Scholarship and Teaching, and the Department of Geology at Miami University. We thank the Ethiopian Mapping Agency and the NASA Goddard Space Flight Center for imagery. We thank H. Gilbert for fieldwork and for work on the illustrations. D. Brill made the photographs and G. Richards and B. Plowman at the University of Pacific made the scanning electron microscope (SEM) image. T. Larson provided invaluable field and laboratory geology support. A. Defleur assisted in field survey and excavations at BOU-VP-11. We thank H. Saegusa for proboscidean identifications, D. DeGusta for primate identifications and excavations at BOU-VP-12/1, and F. C. Howell for carnivore identifications. We thank O. Lovejoy, G. Suwa, and B. Asfaw for helpful comments. We thank the Ethiopian Ministry of Information and Culture, the Centre for Research and Conservation of the Cultural Heritage, and the National Museum of Ethiopia. We thank the Afar Regional Government and the Afar people of the Middle Awash for permission and support. We thank the many individuals who contributed to the camp, transport, survey, excavation, and laboratory work that stands behind the results presented.

25 February 1999; accepted 30 March 1999

Australopithecus garhi: A New Species of Early Hominid from Ethiopia

Berhane Asfaw,¹ Tim White,^{2*} Owen Lovejoy,³ Bruce Latimer,^{4,5} Scott Simpson,⁵ Gen Suwa⁶

The lack of an adequate hominid fossil record in eastern Africa between 2 and 3 million years ago (Ma) has hampered investigations of early hominid phylogeny. Discovery of 2.5 Ma hominid cranial and dental remains from the Hata beds of Ethiopia's Middle Awash allows recognition of a new species of *Australopithecus*. This species is descended from *Australopithecus afarensis* and is a candidate ancestor for early *Homo*. Contemporary postcranial remains feature a derived humanlike humeral/femoral ratio and an apelike upper arm-to-lower arm ratio.

The succession of early hominid genera and species indicates diversification into at least two distinct adaptive patterns by ~2.7 Ma. A meager east African hominid record between 2 and 3 Ma has caused the pattern and pro-

cess of this diversification to remain obscure. The *Australopithecus afarensis* (3.6 to 3.0 Ma) to *A. aethiopicus* (2.6 Ma) to *A. boisei* (2.3 to 1.2 Ma) species lineage is well corroborated by craniodental remains. In contrast, a suggested relationship between *A. afarensis* and early *Homo* has previously been evidenced only by relatively uninformative isolated teeth (1), a palate (2), and a temporal fragment (3).

The recovery of hominid remains from the Hata (abbreviation of Hatayae) Member of the Bouri Formation adds substantially to the inventory of fossils bearing on these phylogenetic issues. These remains comprise craniodental and postcranial elements from several areas in the Middle Awash. The first of these was discovered in 1990 at Matabaietu and Gamedah.

¹Rift Valley Research Service, Post Office Box 5717, Addis Ababa, Ethiopia. ²Laboratory for Human Evolutionary Studies, Museum of Vertebrate Zoology, and Department of Integrative Biology, University of California at Berkeley, Berkeley, CA 94720, USA. ³Department of Anthropology and Division of Biomedical Sciences, Kent State University, Kent OH 44242, USA. ⁴Cleveland Museum of Natural History and ⁵Department of Anatomy, School of Medicine, Case Western Reserve University, Cleveland, OH 44106, USA. ⁶University Museum, University of Tokyo, Hongo, Bunkyo-ku, Tokyo, 113-0033, Japan.

*To whom correspondence should be addressed. E-mail: timwhite@socrates.berkeley.edu

REPORTS

Biochronology and Ar/Ar dating place these remains at ~2.5 Ma. They include a small left parietal fragment (GAM-VP-1/2) and an edentulous left mandible corpus from Gamedah (GAM-VP-1/1), as well as a distal left humerus from Matabaietu (MAT-VP-1/1). It is impossible to attribute the humerus and parietal fragments to a genus. However, the small, fluvially abraded Gamedah mandible retains tooth roots and corpus contours. These demonstrate that it is not a robust *Australopithecus*.

It was not until 1996–1998 that we recovered additional hominid remains of comparable antiquity west of the modern Awash, at Bouri. The proximal half of an adult hominid ulna (BOU-VP-11/1) was found on the surface of the Hata beds by T. Assebework on 17 November 1996. On 30 November, White found a proximal femur and associated forearm elements of a smaller individual, ~100 m to the WNW (BOU-VP-12/1A-G). Sieving and excavation revealed additional portions of this individual's femur in situ, 1 m above a 2.496 Ma volcanic ash, in a horizon with abundant catfish remains and medium-sized bovid fossils, the latter bearing cut marks (4).

This partial hominid skeleton includes fairly complete shafts of a left femur and the right humerus, radius, and ulna. A partial fibular shaft, a proximal foot phalanx, and the base of the anterior portion of the mandible were also found. There is no evidence that these remains represent more than one individual. Except for the in situ distal femoral shaft segment, all were surface finds lying within 2 m of one another. All are similarly preserved. Lengths can be accurately estimated for the phalanx, the femur, and the three arm elements. The foot phalanx is similar to remains of *A. afarensis* in size, length, and curvature. The mandible does not retain diagnostic morphology. No associated hominid teeth were found on the surface or in a large excavation.

Further search of the same ~2.5 Ma horizon led to the discovery, 278 m farther NNW, of a partial hominid cranium (BOU-VP-12/130) on 20 November 1997 by Y. Haile-Selassie (Fig. 1). Another individual's crested cranial vault fragment (BOU-VP-12/87) was found 50 m south of the BOU-VP-12/1 skeleton excavation. At a more northerly locality in the Esa Dibo area ~9 km away, A. Defleur found a fairly complete mandible, with dentition, of another hominid individual (BOU-VP-17/1) on 17 November 1997. An additional hominid humeral shaft (BOU-VP-35/1) was found ~1 km farther north of the location of the mandible, on 4 December 1998, by D. DeGusta. On biochronological grounds, these Esa Dibo specimens are about the same age as the more southerly cluster of hominid remains at Bouri localities 11 and 12 (4).

Great uncertainty has continued to confound the origin of *Homo* because of a lack of evidence from the interval between 2 and 3

Ma (5). The 2.5 Ma Bouri Hata hominids bear directly on these issues. In addition, they are closely associated with behavioral evidence of lithic technology (4). *Australopithecus africanus* from South Africa is roughly contemporary with the Hata remains. In eastern Africa, *A. aethiopicus* and at least one other putative lineage ancestral to early *Homo* are contemporaries in the Turkana Basin. The BOU-VP-12/130 cranial remains represent no previously named species. Only the recovery of additional specimens with associated crania and dentitions may allow the Bouri postcrania to be positively attributed to this new taxon. Therefore, the new species described below is established strictly on the basis of craniodental remains.

The following is a description of *Austra-*

lopithecus garhi, based on the BOU-VP-12/130 specimen: order, Primates Linnaeus 1758; suborder, Anthropoidea Mivart 1864; genus, *Australopithecus* DART 1925; and species, *Australopithecus garhi*.

Etymology. The word *garhi* means “surprise” in the Afar language.

Holotype. ARA-VP-12/130 is an associated set of cranial fragments comprising the frontal, parietals, and maxilla with dentition. It was found by Y. Haile-Selassie on 20 November 1997. The holotype is housed at the National Museum of Ethiopia, Addis Ababa.

Locality. Bouri Vertebrate Paleontology locality 12 (BOU-VP-12) is on the eastern side of the Bouri peninsula, west of the modern Awash River, in the Middle Awash paleoanthropological study area, Afar depres-



Fig. 1. Cranial parts of BOU-VP-12/130. **(Top)** Superior view of the original fossil. Nonstandard orientation (rotated posteriorly ~10° from Frankfurt horizontal) to show maximum anatomy. **(Bottom)** Lateral view of casts to show cranial and maxillary profiles. Note that neither Frankfurt horizontal nor placement of the maxilla relative to the vault can be accurately determined and that reconstructed portions (indicated by oblique lines) are speculative. Photos ©David L. Brill 1999/Atlanta.

REPORTS

sion, Ethiopia. The BOU-VP-12/130 holotype was found at 10°15.6199'N, 40°33.8445'E, at ~550 m elevation.

Horizon and associations. The holotype was recovered from silty clays within 2 m of the top of the Maoleem vitric tuff, which has been dated to 2.496 Ma by Ar/Ar. Vertebrate fossils, including additional hominids, were found at the same stratigraphic horizon on nearby outcrops (4).

Diagnosis. *Australopithecus garhi* is a species of *Australopithecus* distinguished from other hominid species by a combination of characters presented in Table 1. It is distinguished from *A. afarensis* by its absolutely larger postcanine dentition and an upper third premolar morphology with reduced mesio-buccal enamel line projection and less occlusal asymmetry. *Australopithecus garhi* lacks the suite of derived dental, facial, and cranial

features shared by *A. aethiopicus*, *A. robustus*, and *A. boisei*. *Australopithecus garhi* is distinguished from *A. africanus* and other early *Homo* species by its primitive frontal, facial, palatal, and subnasal morphology.

Dental description. The postcanine dental size is remarkable, at or beyond the known nonrobust and *A. robustus* extremes (Fig. 2). The anterior dentition is also large, with I1 and canine breadths equivalent to or exceed-

Table 1. List of characters. Listed are characters widely used in consideration of hominid phylogenetics (11, 13) that are preserved on the BOU-VP-12/130 holotype cranium. Because of arbitrary boundaries of presence or absence criteria, variability within species, limited sample sizes, and possible correlation between features, we caution against a numerical cladistic application of these tabulated data. Rather, this character list is meant to demonstrate the phenetic status of the single known *A. garhi* specimen with respect to features used to

evaluate early hominid fossils. Note that despite the large postcanine dentition, no shared derived characters link *A. garhi* with *A. robustus* or *A. boisei*. The "early *Homo*" column comprises specimens assigned by various authors to both *H. habilis* and *H. rudolfensis*. Abbreviations are as follows: mod., moderate; asym., asymmetric; disp., disparate; sym., symmetric; rect., rectangular; para., parabolic; var., variable; conv., convergent; div., divergent; ant., anterior; prom., prominent; proc., procumbent; cont., continuous; interm., intermediate.

	Males of						
	<i>A. afarensis</i>	<i>A. garhi</i> (n = 1)	Early <i>Homo</i>	<i>A. africanus</i>	<i>A. aethiopicus</i> (n = 1)	<i>A. robustus</i>	<i>A. boisei</i>
<i>Dentition</i>							
Canine to postcanine ratio	large	large	large	large	unknown	small	small
Incisor to postcanine ratio	large	smaller	large	smaller	smaller?	small	small
Postcanine absolute size	mod.	large	mod.	mod. to large	large	large	large
UP3 occlusal outline	asym.	more oval	more oval	more oval	oval	oval	oval
UP3 mesiobuccal line extension	frequent	absent	rare	rare	absent	absent	absent
Postcanine PM/M cusp wear	disp.	disp.	disp.	disp.	flat	flat	flat
Canine lingual shape	asym.	asym.	asym.	asym.	unknown	more sym.	more sym.
Premolar molarization	none	minor	minor	minor	pronounced	pronounced	pronounced
Enamel thickness	moderately thick	thick	thick	thick	hyperthick	hyperthick	hyperthick
<i>Palate</i>							
Ant. vertical thickness	thin	thin	thin	thin	thick	thick	thick
Dental arcade shape	rect.	rect.	para.	var.	rect.	para.	para.
Posterior dental arcade	conv.	div.	div.	div.	conv.	div.	div.
Ant. depth	shallow	shallow	deep	var.	shallow	usually deep	deep
UI2/UC diastema	common	present	rare	absent	absent	absent	absent
Incisor alveoli relative to bicanine line	ant.	ant.	var.	ant.	in line	in line	in line
<i>Lower face</i>							
C jugum	prom.	prom.	var.	prom.	weak	weak	weak
Ant. pillars	absent	absent	absent	present	absent	present	absent
Inferolateral nasal aperture margin	sharp	sharp	sharp	var.	blunt	var.	var.
UI2 root lateral to nasal aperture	lateral	in line	medial	medial	medial	medial	medial
Canine fossa	present	present	var.	present	absent	absent	absent
Maxillary fossula	absent	absent	absent	absent	absent	present	absent
Anterior zygomatic root position	M1	M1-P4	M1-P4	M1-P4	P4	P4-P3	P4/M1-P3
Zygomatocoalveolar crest	arched	arched	arched	var.	weak	var.	var.
Clivus contour	convex	convex	flat/convex	flat	concave	flat to concave	flat to concave
Subnasal prognathism	strong	strong	var.	var.	strong	weak	weak
Incisor procumbency	proc.	proc.	var.	var.	proc.	more vertical	more vertical
Subnasal to intranasal contours	discrete	discrete	discrete	var.	cont.	cont.	var.
Separation of vomeral/ant. septal insertion	strong	strong	usually strong	weak	weak	weak	weak
Lateral ant. facial contour	bipartite	bipartite	var.	var.	straight	straight	straight
Facial dishing	absent	absent	absent	absent	dished	dished	dished
<i>Vault</i>							
Frontal trigon	present	present	absent	absent	present	present	present
Costa supraorbitalis	present	present	torus	interm.	present	present	present
Temporal line's frontal convergence	mod.	mod.	weak	weak	strong	strong	strong
Postorbital constriction	mod.	mod.	mod.	mod.	marked	marked	marked
Sagittal crest in male	present	present	rare	rare	present	present	present
Relative size of posterior temporalis	large	interm.	interm.	interm.	large	small	small
Parietal transverse expansion/tuber	absent	absent	present	absent	absent	absent	absent
Parietomastoid angle	flared	weak	weak	weak	flared	weak	weak
Cranial capacity	small	small	enlarged	small	small	slightly enlarged	slightly enlarged

ing those of their largest known *Australopithecus* and early *Homo* homologs. Thus, despite exceptional postcanine size, dental proportions of the holotype deviate markedly from the robust *Australopithecus* condition. The canine-to-premolar/molar size ratios are comparable to those of *A. afarensis*, *A. africanus*, and early *Homo*. Relative canine to incisor alveolar length is most similar to that of *A. africanus*. Postcanine wear, with developed angular facets and retention of buccal cusp saliency, differs distinctively from the robust *Australopithecus* pattern. The upper P3 is more derived than that of *A. afarensis* and most *A. africanus* specimens in exhibiting a reduced mesiobuccal crown quadrant and a weak transverse crest. The buccolingual narrowing of premolars and first molars often seen in early *Homo* is absent.

Cranial description. The lower face is prognathic, with procumbent incisors. Canine roots are placed well lateral to the nasal aperture margin. The premaxillary surface is separated from the nasal floor by a blunt ridge and is transversely and sagittally convex. The palate is vertically thin (~3 mm at M1/M2 midline). The zygomatic roots originate above P4/M1. The dental arcade is U-shaped, with slightly divergent dental rows (Fig. 3). The temporal lines encroach deeply on the frontal, past the midsupraorbital position, and probably met anterior to bregma. The postglabellar frontal squama is depressed in a frontal lobe. The localized frontal sinus

is limited to the medial one-third of the supraorbital surface. Postorbital constriction is marked. The parietal bones have a well-formed, bipartite, anteriorly positioned sagittal crest that divides above lambda. An endocast was made from the aligned parietals and frontal and was completed by sculpting by R. Holloway. Cranial capacity was about 450 cm³, as measured by water displacement.

Taxonomic discussion. There is no current agreement about how many pre-*erectus* *Homo* species should be recognized or even on how the genus *Homo* should be defined. The traditional conservative definition emphasizes adaptive plateau. Ironically, by this definition, the early *Homo* species *H. rudolfensis* and *H. habilis* might be better placed in *Australopithecus*, as this would affiliate the major adaptive breakthroughs in anatomy and behavior that characterize *H. erectus* (*ergaster*) with the earliest defined occurrence of *Homo*. If *A. garhi* proves to be the exclusive ancestor of the *Homo* clade (see discussion below), a cladistic classification might assign it to genus *Homo*. Here we provisionally adopt the conservative, grade-sensitive alternative, emphasizing its small brain and large postcanine dentition by assigning the new Bouri species to *Australopithecus*. This attribution as well as our diagnosis and description may require emendation when additional individuals representing the species are recovered and firm postcranial associations are established (6).

Although the Bouri Hata postcrania cannot

presently be assigned to the new species *A. garhi*, they illuminate aspects of hominid evolution. The past few years have witnessed a rash of attempts to estimate early hominid limb length proportions from fragmentary and unassociated specimens. These specimens have been used to generate a variety of functional and phylogenetic scenarios. Accurate estimates of the limb proportions of early hominids, however, must be confined to the very few specimens that actually preserve relevant elements, such as the A.L. 288-1 ("Lucy") specimen and KNM-WT 15000. The new Bouri VP-12/1 specimen is only the third Plio-Pleistocene hominid to provide reasonably accurate limb length proportions. The Olduvai Hominid 62 specimen of *Homo habilis* has been erroneously argued to show humerus-to-femur proportions more primitive than those of "Lucy" (7, 8), but its femur length cannot be accurately estimated. Other studies of limb proportions in early *Australopithecus* species are based on unassociated joints and not on actual (or even estimated) limb lengths (7).

The postcranial remains recovered from BOU-VP-11, -12, and -35 cannot be conclusively allocated to taxon. The BOU-VP-12/1 specimen features a humanlike humeral/femoral ratio (Fig. 4). This ratio may be an important derivation relative to *A. afarensis*, because it marks the earliest known appearance of the relative femoral elongation that characterizes later hominids. However, as in *A. afarensis*, the specimen's brachial index is

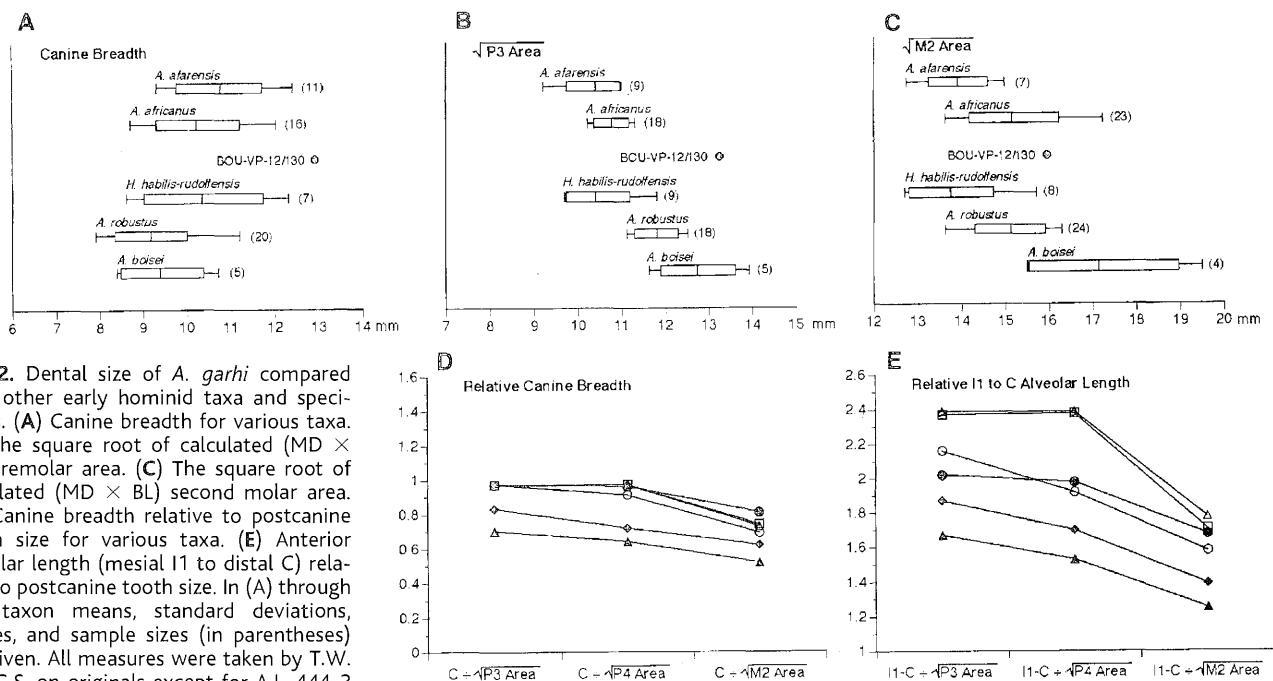


Fig. 2. Dental size of *A. garhi* compared with other early hominid taxa and specimens. (A) Canine breadth for various taxa. (B) The square root of calculated (MD × BL) premolar area. (C) The square root of calculated (MD × BL) second molar area. (D) Canine breadth relative to postcanine tooth size for various taxa. (E) Anterior alveolar length (mesial I1 to distal C) relative to postcanine tooth size. In (A) through (C), taxon means, standard deviations, ranges, and sample sizes (in parentheses) are given. All measures were taken by T.W. and G.S. on originals except for A.L. 444-2 and A.L. 417-1 (*A. afarensis*) and A.L. 666-1 (*Homo*), which are from (2, 14). Dental metrics for the BOU-VP-12/130 specimen are as follows (XX broken; parentheses = estimate; mesiodistal measure reported first, followed by buccolingual): R1 XX, (9.2); R2 6.9, 6.8; RC 11.6, 12.9; RP3 (11.0), 16.0; RP4 XX, XX; RM1 XX, XX; RM2 (14.4), (17.7); RM3 (15.2), 16.9; LI2 6.7, 7.0; LC 11.7, 12.9; LP3 (11.4), 16.0; LP4 (11.4), 16.0; LM1 (14.4), (16.5). □, *A. afarensis*; ○, *A. africanus*; △, *Homo*; ◆, *A. robustus*; ▲, *A. boisei*; ●, BOU-VP-12/130.

REPORTS

apelike. This suggests that upper arm-to-lower arm ratios persisted into the basal Pleistocene and that the first hominid with modern forearm proportions was probably *Homo erectus* (*ergaster*). Because the *A. afarensis* forearm was also long relative to both the humerus and femur, the femur must have elongated before forearm shortening in early hominids.

The BOU-VP-11 ulna is from a larger individual, as is the BOU-VP-35/1 humeral shaft (estimated total humeral length = 310 to 325 mm). The latter is absolutely longer than the humerus of BOU-VP-12/1 but is less rugose and probably bore a smaller deltopectoral crest. These differences (in both size and rugosity) are well within the species ranges of extant hominoids. If both humeri represent the same taxon, they could reflect sexual dimorphism, which would be comparable to that currently seen in *A. afarensis*. However, it is perilous to speculate on differences between only two specimens as they may reflect only fluctuating intraspecific variation in morphology and body mass.

The few and fragmentary nonrobust Turkana Basin hominids that span the 2.7 to 2.3 Ma time range are similar to the Bouri specimens in both size and aspects of morphology. Postca-

nine dental arcade length of BOU-VP-12/130 is equivalent to that of Omo 75-14, whereas individual teeth of the smaller Middle Awash mandibles (GAM-VP-1/1 and BOU-VP-17/1) are comparable in size to the smaller specimens of the Omo nonrobust collection. It is also important that BOU-VP-17/1 exhibits a derived lower P3 morphology (1) most similar to the Omo nonrobust and early *Homo* conditions and a dental arcade shape concordant with that of the holotype of *A. garhi*.

On the basis of size, BOU-VP-12/130 is a male. The craniodental size dimorphism documented for the closely related *A. afarensis* and *A. boisei* therefore predicts smaller individuals in *A. garhi*. The biochronologically contemporary and morphologically compatible BOU-VP-17/1 and GAM-VP-1/1 specimens are considerably smaller and may be females. This would suggest a shift in either or both body and dentognathic sizes to averages greater than in *A. afarensis*. More specimens are needed to test this hypothesis.

The discovery of *A. garhi* provides a strong test of many phylogenetic hypotheses that have addressed the relationships among Plio-Pleistocene hominid taxa. The South African species *A. africanus* was once widely considered to be the most primitive hominid. Discoveries of *A.*

afarensis at Hadar and Laetoli displaced *A. africanus*. This more primitive sister species (*A. afarensis*) was in turn supplanted when the increasingly older and more primitive sister taxa *A. anamensis* (9) and *Ardipithecus ramidus* (10) were identified. However, the geometry of post-*afarensis* hominid phylogeny continues to be the focus of debate.

The position of *A. africanus* relative to the emergence of the genus *Homo* has been particularly difficult to resolve, even in the face of unduly elaborate phylogenetic analyses (11). One reason for this difficulty is the fundamental disagreement on whether early *Homo* comprises one sexually dimorphic (*H.*

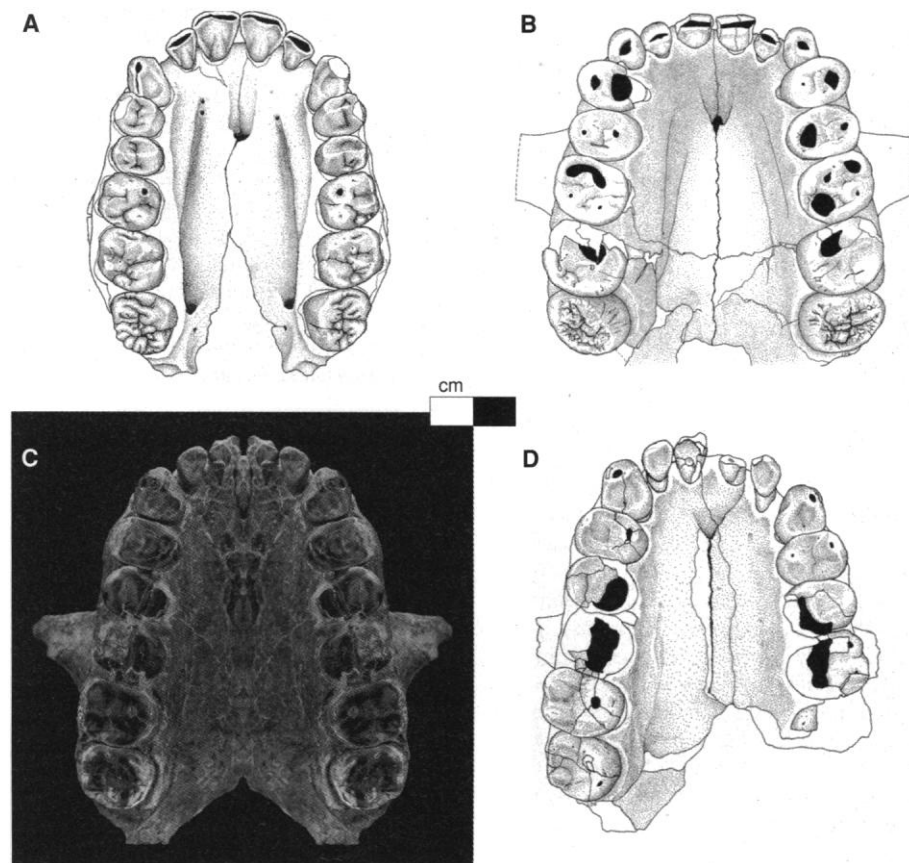


Fig. 3. The most complete palates of *A. afarensis* (A.L. 200-1a; canine reset) (A) and *A. boisei* (OH-5) (B) compared with that of *A. garhi* (C and D). The photograph (©David L. Brill 1999/Atlanta) was mirror-imaged on midline. *Australopithecus garhi* has relatively large canines like *A. afarensis* and absolutely large but morphologically nonrobust premolars and molars. Drawings ©L. Gudz.

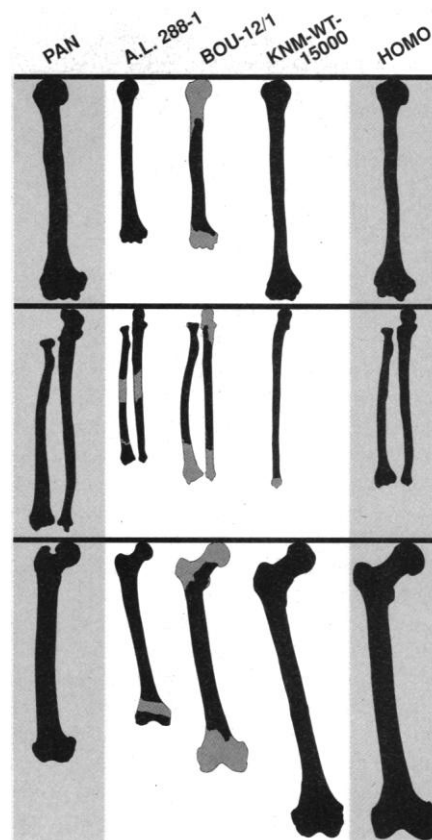
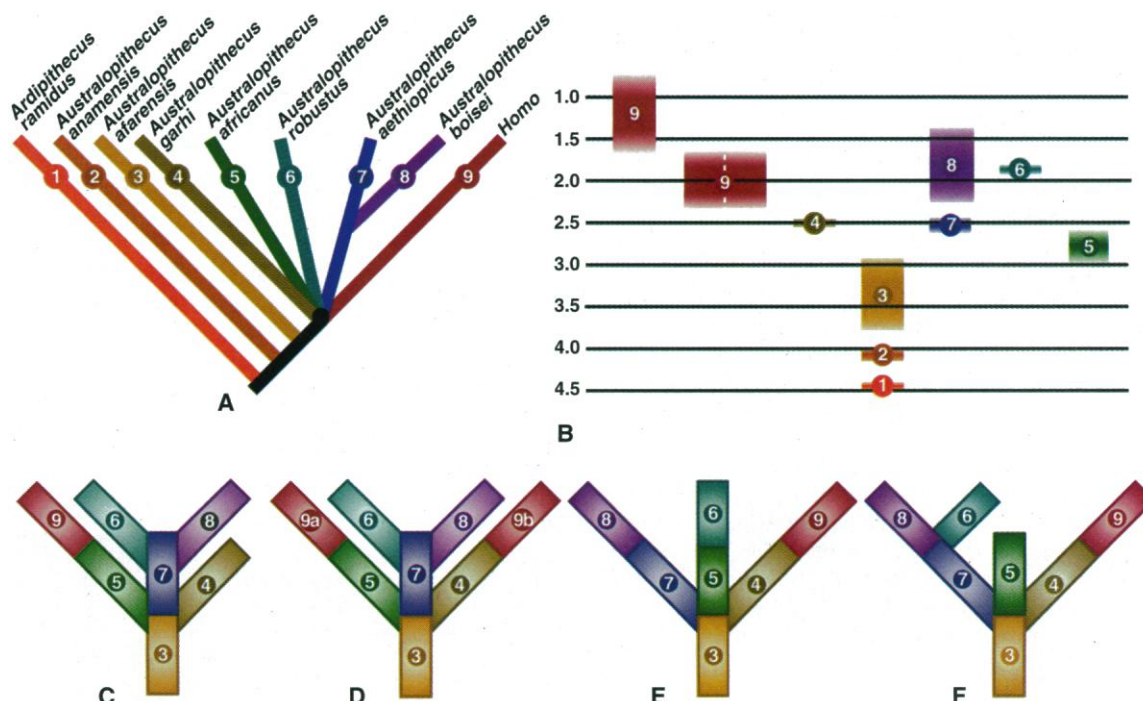


Fig. 4. Probable stages in the progressive differentiation of hominid long bone proportions (all bones shown to the same scale). The humerus (top), antebra-chium (middle), and femur (bottom) are of about equal length in chimpanzees (*Pan*). Modern humans differ in two primary ways. Although our humerus is virtually the same length, the femur is elongated and the antebra-chium is shortened. These changes appear to have emerged fully by ~1.5 Ma in *H. erectus* [all three limb segments are virtually complete in KNM-ER-15000 (15)]. On the basis of the other two partial skeletons in which long bone length can now be reliably estimated, the modern human pattern appears to have emerged in two stages: (i) elongation of the femur, which is intermediate in length relative to the humerus in A.L. 288-1 but exhibits modern proportions in BOU-VP-12/1; and (ii) shortening of the antebra-chium, which retains primitive proportions in both specimens (16). Drawings ©L. Gudz.

REPORTS

Fig. 5. (A) A cladogram depicting relationships among widely recognized early hominid taxa, including the new species *A. garhi*. Note that an additional clade is required when two contemporary forms of early *Homo* are recognized. A variety of possible cladograms have been generated from the data available in the hominid fossil record, but none of these satisfactorily resolve the polychotomy illustrated here (11). This cladogram adds *A. garhi* to the unresolved node. **(B)** The chronological relationships of early hominid taxa. Age is given in Ma. **(C to F)** Alternative phylogenies depicting possible relationships among early hominid taxa. Note that these alternatives do not exhaust the possibilities and that not all are entirely consistent with the cladogram. It is not presently possible to choose among these alternatives.



habilis) or two (*H. habilis* and *H. rudolfensis*) species. Most phylogenetic efforts have placed *A. africanus* as the link between *A. afarensis* and early *Homo*. This hypothesis has been widely, but not universally, accepted. Most predicted that a population of *A. africanus* would be found in eastern Africa when the 2.5 Ma gap there was filled by fossil discoveries.

The 2.5 Ma *A. garhi* is derived toward megadontia from *A. afarensis*, but in cranial anatomy it is definitively not *A. africanus*. Neither is it a representative of the contemporary *A. aethiopicus*. It is in the right place, at the right time, to be the ancestor of early *Homo*, however defined. Nothing about its morphology would preclude it from occupying this position. The close spatial and temporal association between *A. garhi* and behaviors thought to characterize later *Homo* provide additional circumstantial support. The temporal and possible phylogenetic placements of various hominid taxa relative to the new species from Bouri are reviewed in Fig. 5.

Plio-Pleistocene hominid phylogenetics is bedeviled by atomization of functionally correlated character complexes that probably emanate from restricted genomic shifts as well as inadequate fossil samples (particularly for early *Homo*). Table 1 compiles characters available for *A. garhi* and related taxa bearing on phylogenetic placement. The discovery of the KNM-WT 17000 specimen of *A. aethiopicus* demonstrated the pervasiveness of homoplasy in hominid evolution (12). Specimens such as KNM-ER 1590, KNM-ER 1470, KNM-ER 1802,

Malawi UR 501, and Omo 75-14 make it obvious that some early *Homo* specimens exhibit megadontia evolved in parallel with robust *Australopithecus*. *Australopithecus garhi* is certainly megadont, at least relative to craniofacial size. However, its lack of derived robust characters leaves it as a sister taxon to *Homo* but absent many derived *Homo* characters. A strictly cladistic analysis of available data has continually failed to resolve the issue of the position of *A. africanus* (11). The resulting currently unresolved polychotomy (Fig. 5) stems from the fact that those characters most widely used in early hominid phylogenetic systematics are predominantly related to masticatory adaptation and are known to be both interdependent and susceptible to parallel evolution. Other characters such as cranial base flexion and craniofacial hafting are even more poorly understood. The atomization of such morphological complexes has led to lengthy trait lists, but the valence of the individual "characters" is clearly compromised. Such exercises have been useful in establishing the extensive homoplasy present among early hominids, but such confirmation only accentuates the precarious nature of phylogenetic reconstructions based on an incomplete and highly fragmentary fossil record.

Even a combination of all available temporal, spatial, and (circumstantial) behavioral evidence fails to resolve whether the origin of *Homo* was from South African *A. africanus* or east African *A. afarensis* (or both). We now know that a nonrobust species derived from *A. afarensis* persisted in eastern Africa until at least 2.5 Ma. Only additional fossils will con-

firm whether this form participated in a rapid evolutionary transition or transitions resulting in an early form or forms of *Homo*. Such rapid transition may be signaled by the recently described A.L. 266-1 palate from Hadar deposits that are claimed to be 2.33 Ma (2). This palate is more derived than that of *A. garhi*. If *A. garhi* is the direct ancestor of early *Homo*, as represented by such younger specimens as KNM-ER 1590 and KNM-ER 1470, additional major craniofacial changes must have occurred after 2.5 Ma, many of them as direct consequences of brain enlargement. Novel behavioral shifts associated with meat and marrow procurement by means of lithic technology may have played instrumental selective roles during this critical and perhaps short period of evolution.

References and Notes

1. G. Suwa, T. D. White, F. C. Howell, *Am. J. Phys. Anthropol.* **101**, 247 (1996).
2. W. H. Kimbel et al., *J. Hum. Evol.* **31**, 549 (1996); D. C. Johanson and Y. Rak, *Am. J. Phys. Anthropol.* **103**, 235 (1997).
3. A. Hill, S. Ward, A. Deino, G. Curtis, R. Drake, *Nature* **355**, 719 (1992).
4. J. de Heinzelin et al., *Science* **284**, 625 (1999).
5. B. A. Wood, *Nature* **355**, 783 (1992).
6. The Chameron temporal (3) has been called the earliest *Homo*, but the only two characters cited in support of this attribution (a medially positioned mandibular fossa and a sharp petrous crest) are missing from the Bouri holotype, and neither provides unambiguous evidence of brain expansion. Only additional discoveries will test whether Chameron is a Kenyan representative of *A. garhi*.
7. H. M. McHenry and L. R. Berger, *J. Hum. Evol.* **35**, 1 (1998).
8. S. Hartwig-Scherer and R. D. Martin, *ibid.* **21**, 439 (1991).

9. M. G. Leakey, C. S. Feibel, I. McDougall, A. C. Walker, *Nature* **376**, 565 (1995).
10. T. D. White, G. Suwa, B. Asfaw, *ibid.* **371**, 306 (1994); *ibid.* **375**, 88 (1995).
11. A. T. Chamberlain and B. A. Wood, *J. Hum. Evol.* **16**, 119 (1987); R. R. Skelton and H. M. McHenry, *ibid.* **23**, 309 (1992); D. S. Strait, F. E. Grine, M. A. Moniz, *ibid.* **32**, 17 (1997); R. R. Skelton and H. M. McHenry, *ibid.* **34**, 109 (1997).
12. F. E. Grine, Ed., *Evolutionary History of "Robust" Australopithecines* (de Gruyter, New York, 1988); A. C. Walker, R. E. Leakey, J. M. Harris, F. H. Brown, *Nature* **322**, 517 (1986); H. M. McHenry, in *Contemporary Issues in Human Evolution*, W. E. Meikle, F. C. Howell, N. G. Jablonski, Eds. (California Academy of Sciences, San Francisco, 1996), pp. 77–92.
13. W. H. Kimbel, T. D. White, D. C. Johanson, *Am. J. Phys. Anthropol.* **64**, 337 (1984); G. Suwa *et al.*, *Nature* **389**, 489 (1997); P. V. Tobias, *Olduvai Gorge, Volume 4: The Skulls, Endocrasts and Teeth of Homo habilis* (Cambridge Univ. Press, Cambridge, 1991).
14. W. H. Kimbel, D. C. Johanson, Y. Rak, *Nature* **368**, 449 (1994).
15. A. C. Walker and R. E. Leakey, Eds., *The Nariokotome Homo erectus Skeleton* (Harvard Univ. Press, Cambridge, MA, 1993).
16. Femur and humerus length were virtually complete in A.L. 288-1 [D. C. Johanson *et al.*, *Am. J. Phys. Anthropol.* **57**, 403 (1982)]. In BOU-VP-12/1, the femur is preserved from the intersection of the medial terminus of the neck with the (missing) femoral head (proximally) to a point on the medial supracondylar line just superior to the gastrocnemius impression (distally). This distance was measured in a sex- and species-balanced sample of *Pan*, *Gorilla*, and *Homo* ($N = 60$) and used to regress (least squares) femoral length [correlation coefficient (r^2) = 0.952; 95% confidence interval of estimate = ± 0.28]. This regression computes the BOU-VP-12/1 femur at 348 mm. On anatomical grounds, we believe it to have actually been slightly shorter (about 335 mm). Much of the shaft of the BOU-12/1 humerus is preserved, including the point of confluence between the diaphysis and the medial epicondylar apophysis and the distalmost extent of the deltopectoral crest. This distance was used to regress humeral length with the same sample (length estimate = 226 mm; $r^2 = 0.876$; 95% confidence interval of estimate = ± 0.40). On anatomical grounds, we estimate the humerus to have been slightly longer (about 236 mm). Radial length was estimated for A.L. 288-1 with multiple linear regressions from the same sample (breadth distal articular surface; maximum diameter radial head; length radial neck; $r^2 = 0.929$; 95% confidence interval of estimate = ± 0.29) and for BOU-VP-12/1 (radial head to nutrient foramen; maximum diameter radial head; length radial neck; $r^2 = 0.937$; 95% confidence interval of estimate = ± 0.27). These regressions estimate a length of 203 mm for A.L. 288-1 and 231 mm for BOU-VP-12/1. On anatomical grounds, the BOU-VP-12/1 estimate appears correct. However, we believe that the A.L. 288-1 radius is underestimated on the basis of a lack of sufficient "anatomical space" with which to accommodate all of the preserved pieces of the bone. A regression limited to a sample of common chimpanzees and bonobos ($N = 36$) estimates a length of 215 mm ($r^2 = 0.529$; 95% confidence interval of estimate = ± 0.36). This result appears more probable. Only exceptionally pronounced errors in any of the above predictions would alter the conclusions made in the legend of Fig. 3, nor are these conclusions altered by regressions based only on single hominoid species.
17. The Middle Awash paleoanthropological project is multinational (13 countries), interdisciplinary research co-directed by B.A., Y. Beyene, J. D. Clark, T.W., and G. WoldeGabriel. The research reported here was supported by the NSF. We thank N. Tahiru and A. Abdo for their assistance in naming the new species. We thank Y. Haile-Selassie for discovery of the BOU-VP-12/130 holotype and H. Gilbert and D. DeGusta for field and illustrations work. R. Holloway kindly allowed us to cite his BOU-VP-12/130 cranial capacity estimate. L. Gudz made the palate and postcranial drawings. D. Brill made the photographs. P. Reno provided comparative primate

data. The Japan Ministry of Education, Science, Sports and Culture provided support to G.S. We thank the Ethiopian Ministry of Information and Culture, the Centre for Research and Conservation of the Cultural Heritage, and the National Museum of Ethiopia. We thank the Afar Regional Government and the Afar people of

the Middle Awash for permission and support. We thank the many individuals who contributed to the camp, transport, survey, excavation, and laboratory work that stands behind the results presented.

25 February 1999; accepted 30 March 1999

Electron Solvation in Finite Systems: Femtosecond Dynamics of Iodide-(Water)_n Anion Clusters

L. Lehr,*† M. T. Zanni,* C. Frischkorn, R. Weinkauff,†
D. M. Neumark‡

Electron solvation dynamics in photoexcited anion clusters of $I^-(D_2O)_n$ and $I^-(H_2O)_{4-6}$ were probed by using femtosecond photoelectron spectroscopy (FPES). An ultrafast pump pulse excited the anion to the cluster analog of the charge-transfer-to-solvent state seen for I^- in aqueous solution. Evolution of this state was monitored by time-resolved photoelectron spectroscopy using an ultrafast probe pulse. The excited $n = 4$ clusters showed simple population decay, but in the $n = 5$ and 6 clusters the solvent molecules rearranged to stabilize and localize the excess electron, showing characteristics associated with electron solvation dynamics in bulk water. Comparison of the FPES of $I^-(D_2O)_n$ with $I^-(H_2O)_n$ indicates more rapid solvation in the H_2O clusters.

A free electron can be trapped by solvent reorientation in polar solvents such as ammonia (1) or water (2). These "solvated" electrons play an important role in condensed phase chemistry, including radiation chemistry, electron transfer, and charge-induced reactivity. A microscopic understanding of the electron-solvent and solvent-solvent interactions that govern electron solvation is therefore a fundamental and challenging problem. These considerations have motivated femtosecond time-resolved studies that have demonstrated rich and complex dynamics after electronic excitation of electrons in water (3, 4).

To gain a complementary perspective on this problem, we studied solvated electron dynamics in finite clusters and compared these results with our understanding of bulk solvation phenomena. We used two-photon anion femtosecond (10^{-15} s) photoelectron spectroscopy (FPES) (5, 6) to study electron solvation dynamics in the mass-selected anion clusters $I^-(D_2O)_n$ and $I^-(H_2O)_n$ in order to address the following questions: (i) What

is a minimum solvent cluster size needed to solvate an electron? (ii) What is a typical time scale for solvent reorientation in a cluster? (iii) What type of solvent motion is involved in electron solvation dynamics?

Aqueous solutions of I^- exhibit broad electronic bands in the ultraviolet (UV) corresponding to electron ejection from I^- into the solvent (7), known as "charge-transfer-to-solvent" (CTTS) states. Excitation of these states is an elegant means of generating solvated electrons, as was first demonstrated by Jortner (8). The dynamics of these states have been investigated by Eisinger (9), Gaudeul (10), Bradforth (11), and their co-workers, all of whom excited the CTTS states to inject an electron into the water and then followed the subsequent electron solvation dynamics by femtosecond absorption spectroscopy. These experimental studies along with simulations by Sheu and Rossky (12) and Staib and Borgis (13) show that excitation of the lowest energy CTTS band results in the generation of fully solvated electrons on a 200-fs time scale (11). Once generated, these electrons thermalize with the solvent molecules, and some are then lost through geminate recombination with the neutral halogen atom over a time scale of tens of picoseconds.

The issue of how the CTTS bands manifest themselves in finite clusters was first addressed in experiments by Johnson and co-workers (14), in which a diffuse absorption band was seen just above the detachment

Department of Chemistry, University of California, Berkeley, CA 94720, USA and Chemical Sciences Division, Lawrence Berkeley National Laboratory, Berkeley, CA 94720, USA.

*These authors contributed equally to this work.

†Permanent address: Institut für Physikalische und Theoretische Chemie, Technischen Universität München, D-85748 Garching, Germany.

‡To whom correspondence should be addressed. E-mail: dan@radon.cchem.berkeley.edu